Improvement in long-term oxidation resistance of AISI 304L by cold working

Valérie Parry, Audrey Col, Céline Pascal

Improvement in long-term oxidation resistance of AISI 304L by cold working

Valérie Parry[1,*], Audrey Col[1], and Céline Pascal[1]

[1]Univ. Grenoble Alpes, CNRS, Grenoble INP*, SIMaP, F-38000 Grenoble, FRANCE
* Institute of Engineering Univ. Grenoble Alpes

e-mail: Valerie.Parry@simap.grenoble-inp.fr

1. INTRODUCTION

The high temperature oxidation resistance of steels is related to their Cr content and microstructural features. Defects such as lattice distortions and vacancies as well as grain boundaries are known to favor the formation of a protective Cr_2O_3 layer during high temperature exposure [1-4]. On the surface of the metallic substrate, they provide nucleation sites for Cr_2O_3 formation. In the bulk, they allow an efficient Cr supply, preventing an Fe enrichment of the oxide scale and as consequence a breakaway oxidation.
In order to decrease the grain size and introduce defects promoting these mechanisms, a surface treatment can be performed before oxidation: mechanical polishing or grinding [5-6], shot-peening [7-8], sandblasting [6,9-10], shot blasting [11]. During oxidation, the deformed zone transforms to numerous fine grains by recrystallization leading to an increased grain boundary density. Therefore, the Cr diffusion is more efficient and the protectiveness of Cr_2O_3 scale is sustained. Moreover, the toughness of the oxide scales formed on strained surfaces is higher and a decrease of spallation during oxidation or cooling down is observed [5,10]. Severe plastic deformations such as cold rolling [9,12], cold swaging, [13], cold drawing [14] result in a complex evolution of the bulk microstructure : (i) deformation induced martensite before the thermal treatment and (ii) martensite reversion and recrystallization during oxidation [4,15].
The present paper is focused on the effect of cold working on oxidation resistance of AISI 304L austenitic stainless steel. Thermogravimetric analyses were performed in O_2 at 830 °C for 312 h. The chemistry and microstructure of the thermal oxide scales grown in these usual breakaway conditions were studied using scanning electron and Raman spectroscopies. The results were discussed in relation with the microstructural evolution of the bulk.

2. EXPERIMENTAL

The commercial 1 mm-thick foil of AISI 304L (EN 1.4307) used in this work was supplied by Goodfellow. The chemical composition obtained by fluorescence spectroscopy analysis and optical emission spectrometry equipped with a gas analyzer is reported in Table 1. In order to study the effect of cold working on steel oxidation resistance, samples were deformed using a tensile machine up to 40 % strain prior to oxidation. The central part of the tensile specimens were cut to 10 x 20 mm^2 dimensions, ground up to 1200 grit with SiC abrasive papers, then cleaned in acetone and ethanol.

Table 1. Chemical composition of austenitic stainless steel AISI 304L (in wt.%)

wt.%	Fe	Ni	Cr	Mn	Si	Co	Cu	Mo	C	S
AISI 304L	Bal.	8.143	17.462	1.724	0.319	0.203	0.355	0.262	0.021	0.002

Oxidation tests were carried out in a SETARAM B24 thermobalance equipped with a CSEvolution controller. The samples were annealed for 312 h (13 days) in O_2 flow (25 $L.h^{-1}$, i.e. a linear flow 0.35 $cm.s^{-1}$ at room temperature) at 830 °C. The oxidizing atmosphere was kept during the heating (rate of 20 $°C.min^{-1}$) and the cooling (natural) stages. The thermogravimetric experiments were repeated two times. After oxidation, the oxidized sample surface was investigated using Scanning Electron Microscopy (SEM Tescan VEGA-II) and Raman spectroscopy (Renishaw RM1000). Cross-sections were prepared using standard metallographic procedure. Microstructural observations were performed using a Field Emission Gun (FEG) SEM Zeiss Ultra 55 equipped with a SSD Bruker X-Ray detector. In order to estimate the effect of cold working on the bulk material during the initial stages of annealing, microstructural observations were performed on both as-received and deformed samples before and after 4 h at 850 °C. The oxidized sample surfaces were ground up to 1200 grit SiC paper and polished up to 1 µm diamond paste. An electrochemical etching was performed in a 60 % HNO_3 solution at 1V in order to reveal the grain boundaries.

3. RESULTS AND DISCUSSION

Evolutions of the sample weight gain versus time for the as-received and cold worked samples oxidized at 830 °C in O_2 are displayed in Figure 1. SEM surface observations after 312 h (13 days) for the as-received sample and after 288 h (12 days) for the cold worked sample are shown in Figure 2. After 12 days of oxidation, the weight gain of the as-received sample was around 0.97 $mg.cm^{-2}$, more than twice higher than the cold worked sample one (0.39 $mg.cm^{-2}$). The mass gain curve of the as-received sample followed a parabolic shape for 6 days then, after 4 days of linear kinetic a sudden increase of the oxidation rate was observed. This transition is characteristic of the breakaway oxidation. This statement is in agreement with the SEM surface observations in Figure 2a) showing the presence of iron-rich nodules. Conversely, the weight gain of the cold worked sample followed a rather parabolic shape (Figure 1). The oxide scale shown in Figure 2b) was smooth and homogeneous and no Fe-rich nodules were observed. These results suggest that a strong cold working has a beneficial effect on the oxidation resistance of AISI 304L at 830°C.

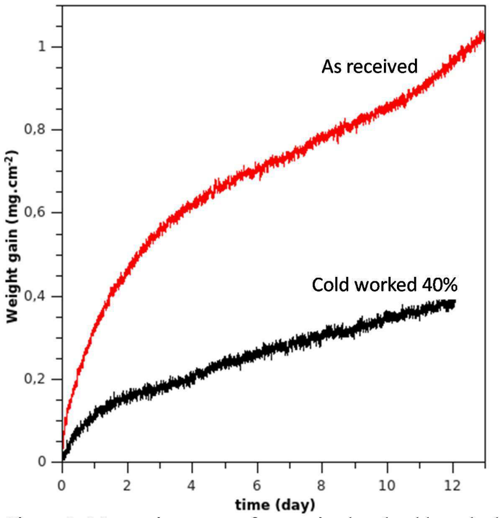

Figure 1: Mass gain curves of as received and cold worked AISI 304L oxidized in O_2 at 830°C.

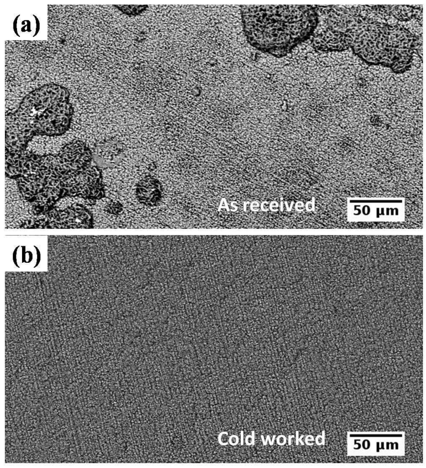

Figure 2: surface SEM images in BSE mode of the oxide scale grown on (a) as received and (b) cold worked AISI 304L samples oxidized in O_2 at 830°C for 312 h and 288 h respectively.

In order to study the protectiveness loss of the Cr rich oxide scale, SEM observations and EDS profiles were performed on cross-sections as well as surface Raman spectroscopy on the as-received and cold worked samples. Results are displayed in Figure 3. For each cross-section, 20 thickness measurements were performed on different SEM images. The thickness of the thermal oxide scale grown on as-received sample was 2.9 ± 0.4 µm whereas the one related to the cold worked sample was slightly thinner (2.1 ± 0.3 µm). For both cases, the oxide scale was duplex: a $(Mn,Cr)_3O_4$ spinel top layer and a Cr_2O_3 inner layer according to Raman spectroscopy and EDS profiles. Whereas the thickness of the inner Cr_2O_3 layer appeared to be similar, the outer layer of the oxide scale grown on the cold worked sample was thinner. This result was supported by Raman spectroscopy where the main contribution related to $MnCr_2O_4$ at 681 cm^{-1} [16] was smaller for the cold worked sample. Cooper et al. also observed that sandblasting and cold rolling decrease the relative amount of spinel for ferritic stainless steels oxidized at 800°C in air for 502 h [9]. Mn is known to diffuse through Cr_2O_3 and form a Mn-rich spinel type oxide at the outer part of the oxide scale. A thinner spinel outermost layer may be the result of a better compactness of the Cr_2O_3 inner layer which limits the transport of scale-forming elements leading to the lower oxide scale thickness.

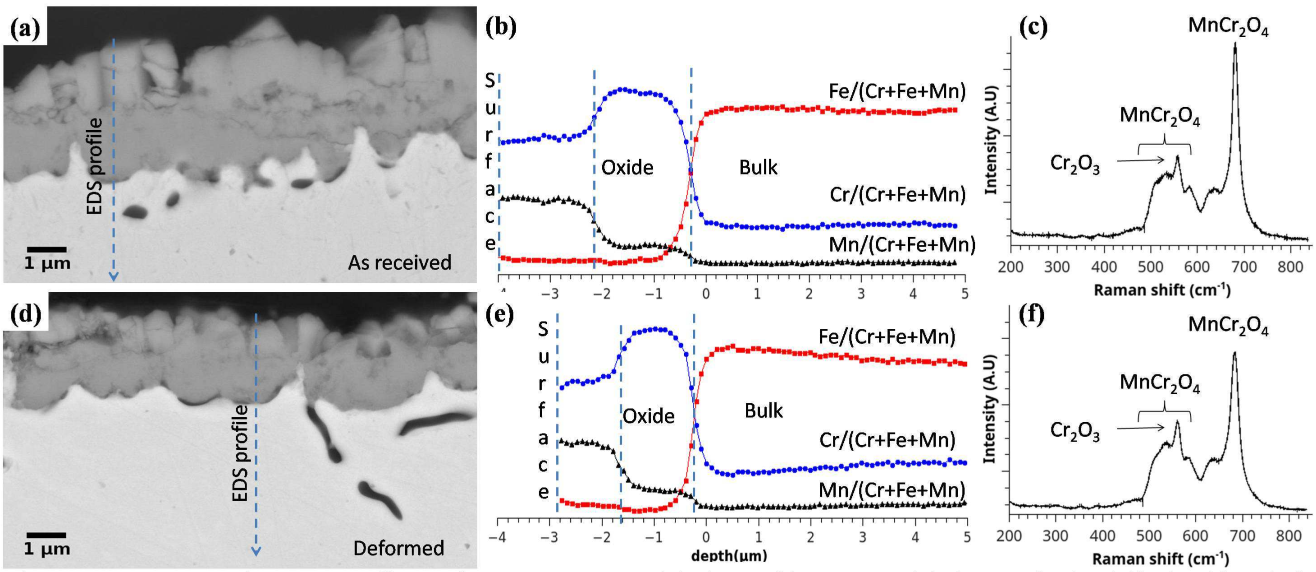

Figure 3: SEM cross sections, EDS profiles, surface Raman spectra of the base oxide grown on (a,b,c) as received and (d,e,f) cold worked AISI 304L samples oxidized in O_2 at 830°C for 312 h and 288 h respectively.

According to EDS profiles in Figure 3, variation of element contents at the alloy/oxide interfaces appeared to be sharp for the cold worked sample. In the substrate beneath the oxide, a short depletion of Cr followed by strong increase was seen whereas a shallow increase of Cr content was observed in the as-received sample. This statement may be linked to an efficient transport of scale-forming elements from the bulk to the oxide in the cold worked sample. In order to explain the better oxidation behavior of the deformed sample, optical observations of the metal surface before oxidation and after 4 h at 850 °C in O_2 were performed on the as-received and deformed samples. Micrographs are presented in Figure 4. According to Figure 4b), the grains were elongated after cold working. After 4 h of oxidation, the grains were equiaxed in both cases (Figure 4 c) and d)). The as-received sample underwent a slight grain growth (Figure 4c)) whereas the grain size decreased for cold worked sample due to recrystallization process (Figure 4d)). In this case, the grain boundary density is high and the diffusion of Cr along the grain boundaries facilitates the early formation of a compact Cr_2O_3 layer leading to the Cr depletion in the underneath metal. However, the Cr supply remains efficient and the protectiveness of Cr_2O_3 scale is sustained.

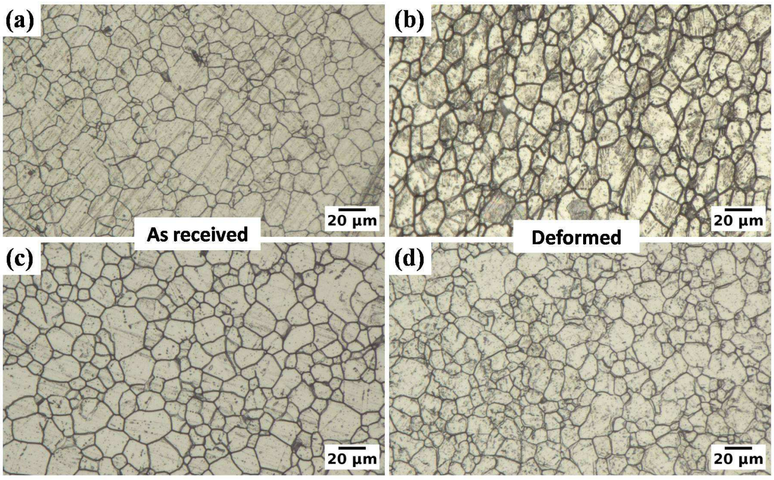

Figure 4: Optical microscopy images of the surface of (a,c) as received and (b,d) cold worked AISI 304L samples (a,b) before and (c,d) after oxidation in O_2 at 850°C for 4 h. The oxide scale was removed by surface polishing

3. CONCLUSION

This study was focused on the effect of cold working on oxidation resistance of AISI 304L austenitic stainless steel at 830 °C in O_2 flow. Thermogravimetric experiments performed for 13 days showed a strong decrease of the oxidation rate of the cold worked sample whereas the as-received sample underwent breakaway oxidation. In order to study the difference in protectiveness of the oxide scale, EDS and Raman chemical analysis were performed on the base oxide. For both cases, the scale was duplex and consisted of a $(Mn,Cr)_3O_4$ spinel outer layer and a Cr_2O_3 inner layer. However, the thermal oxide scale grown on cold worked sample was thinner with a lower spinel amount. This result is probably related to a better compactness of Cr_2O_3 grown on the cold worked sample. The compact Cr_2O_3 limits the transport of scale-forming elements and leads to a reduced overall oxide scale thickness. Analysis of the EDS profiles pointed out a short Cr depletion of a few micron depth in the underneath metallic substrate. This result is linked to the recrystallization process that happens during the early stage of oxidation. For the cold worked sample, the effective diffusion coefficient is higher due the grain boundary contribution promoting an efficient transport of Cr and the sustaining of the Cr_2O_3 protectiveness.

References

[1] Chen, S., Jin, X. & Rong, L. “Improvement in High Temperature Oxidation Resistance of 9 %Cr Ferritic–Martensitic Steel by Enhanced Diffusion of Mn.”*Oxid. Met.*Vol. 85 (2016), pp. 189–203.

[2] Kim, J. H., Kim, D. I., Suwas, S., Fleury, E. & Yi, K. W. “Grain-size effects on the high-temperature oxidation of modified 304 austenitic stainless steel”. *Oxid. Met.* Vol. 79, (2013), pp. 239–247.

[3] Peng, X., Yan, J., Zhou, Y. & Wang, F. “Effect of grain refinement on the resistance of 304 stainless steel to breakaway oxidation in wet air.” *Acta Mater.* Vol. 53 (2005), pp. 5079–5088.

[4] Tomimura, K., Takaki, S., Tanimoto, S. & Tokunaga, Y. “Optimal Chemical Composition in Fe-Cr-Ni Alloys for Ultra Grain Refining by Reversion from Deformation Induced Martensite.” *ISIJ Int.* Vol. 31 (1991), pp. 721–727.

[5] Cissé, S., Laffont, L., Tanguy, B., Lafont, M. C. & Andrieu, E. “Effect of surface preparation on the corrosion of austenitic stainless steel 304L in high temperature steam and simulated PWR primary water”. *Corros. Sci.* Vol. 56, (2012), pp. 209–216.

[6] Ostwald, C. & Grabke, H. J. “Initial oxidation and chromium diffusion. I. Effects of surface working on 9-20% Cr steels.”*Corros. Sci.*Vol. 46 (2004), pp. 1113–1127.

[7] Naraparaju, R., Christ, H. J., Renner, F. U. & Kostka, A. “Effect of shot-peening on the oxidation behaviour of boiler steels.”*Oxid. Met.*Vol. 76 (2011), pp. 233–245.

[8] Yue, Z., Fu, M., Wang, X. & Li, X. “Effect of shot peening on the oxidation resistance of TP304H and HR3C steels in water vapor”. *Oxid. Met.* Vol. 77 (2012), pp. 17–26.

[9] Cooper, L., Benhaddad, S., Wood, A. & Ivey, D. G. “The effect of surface treatment on the oxidation of ferritic stainless steels used for solid oxide fuel cell interconnects.”*J. Power Sources*, Vol. 184 (2008), pp. 220–228.

[10] Yuan, J., Wu, X., Wang, W., Zhu, S. & Wang, F. “The effect of surface finish on the scaling behavior of stainless steel in steam and supercritical water”. *Oxid. Met.* Vol. 79 (2013), pp. 541–551.

[11] Xingeng, L. & Jiawen, H. “Effect of shot blasting on oxidation behavior of TP304H steel at 610–770 °C in water vapor.” *Mater. Let.* Vol. 60 (2006), pp. 339–344.

[12] Lu, Y. H., Wang, Z. B., Song, Y. Y. & Rong, L. J. “Effects of pre-formed nanostructured surface layer on oxidation behaviour of 9Cr2WVTa steel in air and liquid Pb-Bi eutectic alloy.”*Corros. Sci.*Vol. 102 (2016), pp. 301–309.

[13] Chen, S. & Rong, L. “Roles of Mn in the High-Temperature Air Oxidation of 9Cr Ferritic–Martensitic Steel After Severe Plastic Deformation.”*Oxid. Met.*Vol. 89 (2018), pp. 415–428.

[14] Langevoort, J. C., Fransen, T. & Gellings, P. J. “On the influence of cold work on the oxidation of some stainless steels.” *Oxid. Met.* Vol. 21 (1984), pp. 271–284.

[15] Padilha, A. F., Plaut, R. L. & Rios, P. R. “Annealing of Cold-worked Austenitic Stainless Steels”. *ISIJ Int.* Vol. 43, (2003), pp. 135–143.

[16] Farrow, R. L., Benner, R. E., Nagelberg, A. S. & Mattern, P. L. “Characterization of Surface Oxides By Raman Spectroscopy”. *Thin Solid Films.* Vol 73 (1980), pp. 353–358.